

Contents lists available at [ScienceDirect](http://www.sciencedirect.com)

Developmental Biology

journal homepage: www.elsevier.com/developmentalbiology

Functional redundancy of *EGF-CFC* genes in epiblast and extraembryonic patterning during early mouse embryogenesis

Jianhua Chu, Michael M. Shen*

Departments of Medicine and Genetics and Development, Herbert Irving Comprehensive Cancer Center, Columbia University Medical Center, New York, NY 10032, USA

ARTICLE INFO

Article history:

Received for publication 11 November 2009

Revised 25 February 2010

Accepted 16 March 2010

Available online 24 March 2010

Keywords:

Mouse

Nodal signaling

Epiblast

Extraembryonic ectoderm

Visceral endoderm

Anterior–posterior axis

Non-cell-autonomy

ABSTRACT

During early mouse embryogenesis, multiple patterning and differentiation events require the activity of Nodal, a ligand of the transforming growth factor- β (TGF β) family. Although Nodal signaling is known to require activity of EGF-CFC co-receptors in many contexts, it has been unclear whether all Nodal signaling in the early mouse embryo is EGF-CFC dependent. We have investigated the double null mutant phenotypes for the *EGF-CFC* genes *Cripto* and *Cryptic*, which encode co-receptors for Nodal, and have found that they have partially redundant functions in early mouse development. Expression of *Cripto* and *Cryptic* is non-overlapping prior to gastrulation, since *Cripto* is expressed solely in the epiblast whereas *Cryptic* is expressed in the primitive endoderm of the late blastocyst and the visceral endoderm after implantation. Despite these non-overlapping expression patterns, *Cripto*; *Cryptic* double mutants display severe defects in epiblast, extraembryonic ectoderm, and anterior visceral endoderm (AVE), resulting in phenotypes that are highly similar to those of *Nodal* null mutants. Our results indicate that both *Cripto* and *Cryptic* function non-cell-autonomously during normal development, and that most if not all *Nodal* activity in early mouse embryogenesis is EGF-CFC-dependent.

© 2010 Elsevier Inc. All rights reserved.

The Nodal signaling pathway plays a central role in patterning the mouse embryo from pre-gastrulation through early somite stages. In particular, Nodal signaling is required for specification of the anterior–posterior and left–right body axes, as well as formation of the primary germ layers (reviewed in Schier, 2003; Schier and Shen, 2000; Shen, 2007; Whitman, 2001). Furthermore, recent studies have demonstrated that Nodal signaling plays critical roles in multiple patterning and differentiation events at pre-gastrulation stages of development (Brennan et al., 2001; Guzman-Ayala et al., 2004; Mesnard et al., 2006).

Following embryo implantation, *Nodal* is expressed in the epiblast, and mediates reciprocal interactions between the epiblast as well as two adjoining extraembryonic tissues: the visceral endoderm and extraembryonic ectoderm (ExE). Null mutants for *Nodal* display severe defects in all three of these tissues. In the epiblast, *Nodal* mutants display decreased expression of pluripotency markers, suggesting that Nodal signaling is required to maintain the undifferentiated state of the epiblast (Brennan et al., 2001; Mesnard et al., 2006). In the visceral endoderm, Nodal signaling is required for the specification of the distal visceral endoderm (DVE) as well as its subsequent translocation to the prospective anterior side, thereby establishing the anterior–posterior axis (Brennan et al., 2001; Norris

and Robertson, 1999). In the ExE, Nodal signaling is essential for maintenance of the ExE and prevents differentiation of trophoblast stem cells (Brennan et al., 2001; Guzman-Ayala et al., 2004).

Nodal signaling is mediated by an Activin receptor complex composed of a dimer of the type I serine-threonine receptor ALK4 (ActRIB) and a dimeric type II Activin receptor, either ActRII or ActRIIB. Following receptor activation, Smad2 and/or Smad3 are phosphorylated and accumulate together with Smad4 in the nucleus to mediate transcriptional responses (Yan et al., 2002; Yeo and Whitman, 2001) together with the FoxH1 (FAST) winged-helix transcription factor (Chen et al., 1996, 1997), as well as members of the Mixer subfamily of homeodomain proteins (Germain et al., 2000). The Nodal pathway differs from that for Activin in that Nodal signaling requires the activity of EGF-CFC co-receptors (Reissmann et al., 2001; Yan et al., 2002; Yeo and Whitman, 2001), whereas Activin does not require a co-receptor for its signaling activity (Gritsman et al., 1999; Kumar et al., 2001; Yan et al., 2002). EGF-CFC co-receptors are small cysteine-rich extracellular proteins that are attached to the cell membrane by a glycosyl-phosphatidylinositol (GPI) linkage (Shen, 2007; Shen and Schier, 2000; Wechselberger et al., 2005). Two *EGF-CFC* genes are present in the mammalian genome, *Cripto* and *Cryptic*, while a varying number is present in other vertebrate species, including the single zebrafish gene, *one-eyed pinhead* (*oep*).

A central question regarding the function of EGF-CFC proteins has been whether they are essential for all aspects of Nodal signaling, as originally indicated by studies in the zebrafish (Gritsman et al., 1999).

* Corresponding author. Fax: +1 212 851 4572.

E-mail address: mshen@columbia.edu (M.M. Shen).

Analyses of null mutants in the mouse, however, have been less definitive on this issue. Although *Cripto* and *Cryptic* single mutants both display phenotypes associated with defects in Nodal signaling, it has been unclear whether all *Nodal* functions correspond to specific requirements for these EGF-CFC genes. Null mutants for *Cripto* lack embryonic mesoderm and definitive endoderm, and are defective in anterior translocation of the distal visceral endoderm (DVE) (Ding et al., 1998; Xu et al., 1999). In contrast, *Cryptic* null mutants survive until birth and display severe left–right laterality defects, but do not exhibit phenotypes associated with pre-gastrulation patterning and differentiation (Gaio et al., 1999; Yan et al., 1999). Thus, to a first approximation, *Cripto* is required for early Nodal functions prior to and including gastrulation, whereas *Cryptic* is required for later Nodal requirements in left–right specification.

However, null mutants for *Cripto* and *Nodal* display significant differences in their phenotypes (Brennan et al., 2001; Ding et al., 1998; Mesnard et al., 2006), indicating that some Nodal signaling activity is retained in the absence of *Cripto*. In particular, *Cripto* is only expressed in the epiblast, not the visceral endoderm or the ExE, and chimeras with a wild-type visceral endoderm and *Cripto* mutant epiblast still display a *Cripto* null phenotype (Ding et al., 1998; Kimura et al., 2001). Given that *Cripto* functions as a Nodal co-receptor, these observations have led to suggestions that Nodal signaling in the visceral endoderm and ExE may not require EGF-CFC activity (Ben-Haim et al., 2006; Liguori et al., 2008). For example, it has been proposed that signaling by the Nodal precursor from the epiblast to the ExE for maintenance of BMP4 expression is *Cripto*-independent, and possibly EGF-CFC independent as well (Ben-Haim et al., 2006). Similarly, the ability of a *Cerberus-like* (*Cerl*) null mutant to partially rescue the *Cripto* null phenotype has been interpreted as reflecting EGF-CFC-independent Nodal signaling (Liguori et al., 2008). Alternatively, these observations raise the possibility that *Cryptic* may have earlier functions than previously recognized, and also mediates Nodal signaling during early mouse embryogenesis.

In the studies described below, we show that in the absence of *Cripto*, there is an essential role for *Cryptic* in maintenance of the pluripotent epiblast and the extraembryonic ectoderm as well as formation of the distal visceral endoderm. Our findings suggest that EGF-CFC genes are essential for most if not all known aspects of Nodal function in the early mouse embryo.

Materials and methods

Mouse strains and genotyping

The *Cripto* null allele and *Cryptic* null allele used in this study have been previously described (Ding et al., 1998; Yan et al., 1999). The *Nodal-lacZ* mice (Collignon et al., 1996) were generously provided by Liz Robertson.

Genotypes of 5.5, 6.5 and 7.5 dpc whole-mount embryos were determined by PCR using genomic DNA from embryo lysates. Embryos following *in situ* hybridization were similarly genotyped except that a 45-cycle PCR program was used. Genotypes of embryo sections were deduced based on the strict correlation between the mutant phenotypes and their genotypes. PCR primers used were: *Cripto* wild-type (forward) 5'-ACC TGC CCC ATG ACT TCT CTT ACA-3', (reverse) 5'-CCC TGC TGC CCT TAT GCT ATT TTA-3'; *Cripto* mutant (forward) 5'-CCA TCC CCT GCC CGT CTA CAC G-3', (reverse) 5'-GTC ACG CAA CTC GCC GCA CAT-3'; *Cryptic* wild-type (forward) 5'-TTC CTG ACT CCA GCA CTT TGG GA-3', (reverse) 5'-GGC TGA AAA ACA AGT TAG CAG G-3'; *Cryptic* mutant (forward) 5'-GTG GGG GTG GGG TGG GAT TAG AT-3', (reverse) 5'-CCT CTG TTT TTG GTG ACT GTC GC-3'; *Nodal* wild-type (forward) 5'-CCA CTC ACC ATT GAC ATT TTC CAC CAG-3', (reverse) 5'-TGG ATG TAG GCA TGG TTG GTA GGA TG-3'; *Nodal* mutant (forward) 5'-ATA CTG CAC CGG GCG GGA AGG AT-3', (reverse) 5'-CCG CGC TGT ACT GGA GGC TGA AG-3'.

Whole-mount *in situ* hybridization

Whole-mount *in situ* hybridization was performed as previously described (Shen et al., 1997). Mouse probes were as follows: *Afp* (Tilghman et al., 1979); *Bmp4* (Winnier et al., 1995); *Cer1* (*Cerberus-like*) (Belo et al., 1997); *Cdx2* (Strumpf et al., 2005); *Cripto* (Ding et al., 1998); *Cryptic* (Shen et al., 1997); *Hex* (*Hhex*) (Thomas et al., 1998); *Lefty1* (Meno et al., 1997); *Lhx1* (Shawlot and Behringer, 1995); *Mash2* (Guillemot et al., 1994); and *Nanog* (Chambers et al., 2003). The *Oct4* probe corresponded to a 1.0 kb HindIII-AclI fragment amplified from ES cell cDNA and cloned into pBluescript SK. All embryos were genotyped following *in situ* hybridization and photography, except for the embryos used for sectioning.

Results

Non-overlapping expression of *Cripto* and *Cryptic* in the pre-gastrulation embryo

To investigate the potential redundant functions of *Cripto* and *Cryptic*, we first compared their expression at peri-implantation and pre-gastrulation stages of embryogenesis by whole-mount *in situ* hybridization (Fig. 1). In the blastocyst at 3.5 days *post coitum* (dpc), *Cripto* expression can be detected in the inner cell mass, but not the trophectoderm (Fig. 1A). Expression of *Cripto* is later found in the epiblast, but not the primitive endoderm or trophectoderm of the peri-implantation embryo at 4.5 dpc (Fig. 1B). At post-implantation stages, *Cripto* is expressed uniformly in the epiblast at 5.5 dpc, but not in the visceral endoderm or ExE, and is subsequently localized to the proximal epiblast at 6.0 dpc and posterior epiblast and nascent mesoderm at 6.75 dpc (data not shown), as we have previously described (Ding et al., 1998).

In the case of *Cryptic*, we found that expression is first observed in nascent primitive endoderm cells at 4.0 dpc (Fig. 1E). *Cryptic* expression continues in the primitive endoderm and newly formed parietal endoderm of the peri-implantation and early post-implantation embryo at 4.5 and 4.75 dpc (Figs. 1F–H). Expression of *Cryptic* is subsequently found at low levels in the visceral endoderm around the embryonic–extraembryonic boundary at 5.5 dpc (Fig. 1I), and is subsequently up-regulated in the proximal embryonic visceral endoderm and distal extraembryonic visceral endoderm (Fig. 1J). Interestingly, *Cryptic* expression is not uniform within the embryonic visceral endoderm, but instead is expressed preferentially in the anterior visceral endoderm (AVE) (Figs. 1J, K). At early-mid streak stages of gastrulation, *Cryptic* is expressed in nascent mesoderm that will contribute to the axial and lateral mesoderm (Figs. 1K, M), consistent with our previous findings (Shen et al., 1997). Notably, *Cryptic* expression is never observed in the epiblast before gastrulation or in the ExE (Figs. 1I–K, M, N).

These results indicate that the expression patterns of *Cripto* and *Cryptic* do not overlap prior to mesoderm formation. Notably, *Cripto* expression in *Cryptic* null mutants ($n = 2$) is indistinguishable from that in wild-type embryos prior to and during gastrulation (Figs. 1C, D) (Ding et al., 1998). Similarly, *Cryptic* continues to be expressed in *Cripto* null mutants ($n = 2$) at these stages, although *Cryptic* expression is radially symmetric in the visceral endoderm, consistent with the lack of a properly positioned AVE in *Cripto* mutants (Figs. 1L, O). Therefore, there is no evidence for compensatory expression of either *Cripto* or *Cryptic* in the absence of function for the other gene.

Severe post-implantation lethal phenotype of *Cripto*; *Cryptic* double mutants

To investigate EGF-CFC functions in pre-gastrulation development, we analyzed the phenotypes of compound mutants for *Cripto* and *Cryptic* in intercrosses of *Cripto*^{+/-}; *Cryptic*^{+/-} double heterozygotes. At

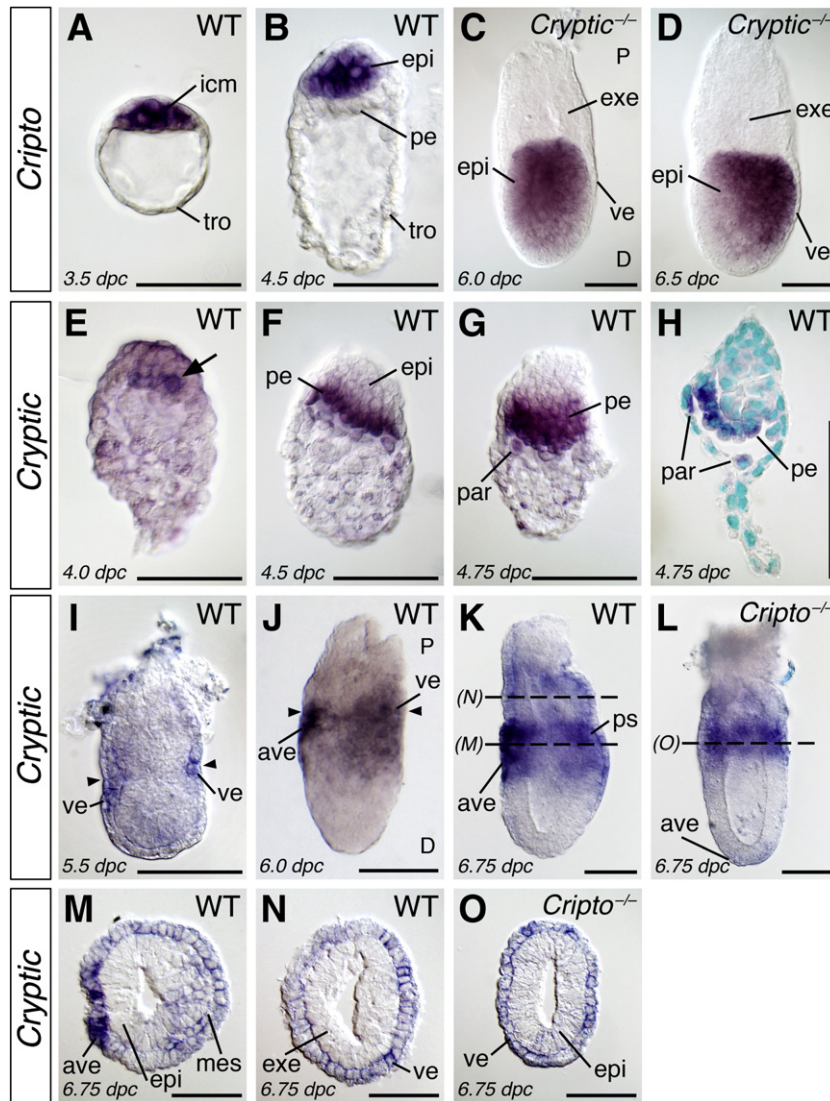


Fig. 1. Expression of *Cripto* and *Cryptic* in mouse embryos at 3.5 to 6.75 days post coitum (dpc). (A–D) *Cripto* expression in wild-type (A, B) and *Cryptic* null mutant (C, D) embryos. (A) Expression of *Cripto* in the wild-type blastocyst at 3.5 dpc is restricted to the inner cell mass, and is not found in the trophectoderm. (B) *Cripto* expression is restricted to the epiblast at 4.5 dpc, and is not found in the primitive endoderm. (C, D) Expression of *Cripto* in the proximal epiblast of a *Cryptic* null mutant at 6.0 dpc (C) and in the posterior epiblast at 6.5 dpc (D) is indistinguishable from the wild-type pattern (Ding et al., 1998). In panel D, proximal (P) and distal (D) are indicated. (E–O) Expression of *Cryptic* in wild-type (E–K, M, N) and *Cripto* null mutant (L, O) embryos. (E) *Cryptic* expression in cells of the nascent primitive endoderm (arrow) at 4.0 dpc. (F, G) Expression of *Cryptic* in the primitive endoderm and newly formed parietal endoderm at 4.5 dpc (F) and 4.75 dpc (G). (H) Longitudinal section of the embryo in (G), showing absence of expression in the epiblast; nuclei are counterstained with methyl green. (I) *Cryptic* expression at 5.5 dpc in the proximal visceral endoderm at the level of the boundary between extraembryonic ectoderm and epiblast (arrowheads). (J) Expression of *Cryptic* at 6.0 dpc in the proximal visceral endoderm, including the anterior visceral endoderm; the junction between extraembryonic ectoderm and epiblast is indicated (arrowheads); proximal (P) and distal (D) are indicated. (K) *Cryptic* expression in the embryonic and extraembryonic visceral endoderm at 6.75 dpc, including the anterior visceral endoderm. (L) Expression of *Cryptic* in the visceral endoderm is unaltered in a *Cripto*^{-/-} embryo at 6.5 dpc. (M, N) Cross-sections of the embryo at the indicated levels in (K), showing *Cryptic* expression in the anterior visceral endoderm, and low-level expression in the visceral endoderm and nascent mesoderm. (O) Cross-section of the embryo in (L). Scale bars correspond to 100 μm. Abbreviations: ave, anterior visceral endoderm; epi, epiblast; exe, extraembryonic ectoderm; icm, inner cell mass; mes, mesoderm; par, parietal endoderm; pe, primitive endoderm; ps, primitive streak; tro, trophectoderm; ve, visceral endoderm.

5.5 dpc, embryos corresponding to all nine possible genotypes can be recovered in Mendelian ratios (Table 1). Morphological examination of the *Cripto*^{-/-}; *Cryptic*^{-/-} double mutant embryos at 5.5 dpc showed that they have a reduced ExE as well as thickened visceral endoderm relative to wild-type as well as *Cripto*^{-/-} single mutants (Figs. 2A, B, D); interestingly, *Cripto*^{-/-} mutants also showed a slightly smaller ExE relative to wild-type (Figs. 2A, B). At 6.5 dpc, *Cripto*^{-/-}; *Cryptic*^{-/-} double mutants lack any evidence of an anterior visceral endoderm, and are significantly smaller than their wild-type or *Cripto*^{-/-} single mutant littermates (Figs. 2G, H, J). By 7.5 dpc, *Cripto*^{-/-}; *Cryptic*^{-/-} embryos are highly abnormal, lacking mesoderm formation or evidence of anterior-patterning, and are in the process of resorbing (Figs. 2M, N, P). Unexpectedly, however, we also found that *Cripto*^{-/-}; *Cryptic*^{+/-}

embryos were phenotypically similar to *Cripto*^{-/-}; *Cryptic*^{-/-} embryos (Table 2; Figs. 2C, I, O), indicating the haploinsufficiency of *Cryptic* in the absence of *Cripto* function; in contrast, *Cripto*^{+/-}; *Cryptic*^{-/-} embryos were phenotypically normal. Furthermore, the phenotypes of both *Cripto*^{-/-}; *Cryptic*^{-/-} and *Cripto*^{-/-}; *Cryptic*^{+/-} embryos were remarkably similar to that of *Nodal*^{-/-} mutants at each stage examined (Figs. 2E, K, Q). Notably, the *Cripto*^{-/-}; *Cryptic*^{-/-} and *Cripto*^{-/-}; *Cryptic*^{+/-} double mutants at 6.5 dpc display an accumulation of visceral endoderm tissue at the distal tip that is characteristic of *Nodal* mutants (Figs. 2I–K).

Given the severe epiblast defects observed in the *Cripto*^{-/-}; *Cryptic*^{-/-} double mutants, we measured the total length of embryos arising from *Cripto*^{+/-}; *Cryptic*^{+/-} intercrosses, as well as for *Nodal*^{-/-} mutants. In

Table 1
Genotypes recovered from *Cripto*^{+/-}; *Cryptic*^{+/-} intercrosses at 5.5 dpc.

Genotype	Recovered	Expected
<i>Cripto</i> ^{+/+} ; <i>Cryptic</i> ^{+/+}	3	4.75
<i>Cripto</i> ^{+/+} ; <i>Cryptic</i> ^{+/-}	9	9.5
<i>Cripto</i> ^{+/+} ; <i>Cryptic</i> ^{-/-}	5	4.75
<i>Cripto</i> ^{+/-} ; <i>Cryptic</i> ^{+/+}	9	9.5
<i>Cripto</i> ^{+/-} ; <i>Cryptic</i> ^{+/-}	20	19
<i>Cripto</i> ^{+/-} ; <i>Cryptic</i> ^{-/-}	12	9.5
<i>Cripto</i> ^{-/-} ; <i>Cryptic</i> ^{+/+}	5	4.75
<i>Cripto</i> ^{-/-} ; <i>Cryptic</i> ^{+/-}	6	9.5
<i>Cripto</i> ^{-/-} ; <i>Cryptic</i> ^{-/-}	7	4.75
Totals	76	

these analyses, we measured the maximal length of the embryo along the proximal-distal axis from the distal tip to the base of the ectoplacental cone, followed by genotyping of the embryos examined (Fig. 2F, L, R). (Because *Cripto*^{-/-}; *Cryptic*^{-/-} or *Cripto*^{-/-}; *Cryptic*^{+/-} embryos have similar phenotypes, these genotypes were grouped together as “*Cripto*; *Cryptic*” embryos). Notably, we found that the embryo lengths of *Cripto*; *Cryptic* double mutants were significantly shorter than that of wild-type or *Cripto*^{-/-} single mutants from 5.5 to 7.5 dpc ($P < 0.01$ for both comparisons at all three stages examined), and were similar to those of *Nodal*^{-/-} single mutants at both 6.5 and 7.5 dpc. These findings indicate that the overall phenotype of *Cripto*; *Cryptic* double mutants is more severe than that of *Cripto* single mutants and is comparable to that of *Nodal* mutants.

Requirement of *Cripto* and *Cryptic* for epiblast and extraembryonic ectoderm maintenance

Based on the defects identified in our morphological analyses, we examined expression of epiblast-specific markers by *in situ* hybridization. The pluripotency marker *Oct4* is expressed in wild-type epiblast at 5.5 and 6.5 dpc (Rosner et al., 1990), but is down-regulated in *Cripto*^{-/-}; *Cryptic*^{-/-} double mutants at 5.5 dpc ($n = 2$) and is absent by 6.5 dpc ($n = 6$) (Figs. 3A, C, D, F). Interestingly, *Oct4* expression in *Cripto*^{-/-} single mutants is relatively normal at 5.5 dpc ($n = 3$), but is also down-regulated or absent at 6.5 dpc ($n = 4$; 3 embryos lacked *Oct4* expression, 1 embryo showed decreased expression) (Figs. 3B, E; data not shown). Furthermore, we found that *Nanog* expression in the posterior epiblast at 6.5 dpc (Morkel et al., 2003) is down-regulated in *Cripto*^{-/-} mutants ($n = 3$), and is absent in *Cripto*^{-/-}; *Cryptic*^{-/-} double mutants ($n = 3$) (Figs. 3G–I). These findings are consistent with a severe epiblast defect in *Cripto*^{-/-}; *Cryptic*^{-/-} double mutants.

To assess the maintenance and differentiation of the ExE, we first examined the expression of *Bmp4*, which marks the ExE proximal to the epiblast in wild-type embryos (Fig. 4A) (Cocouvanis and Martin, 1999). In *Cripto*^{-/-} single mutants, the domain of *Bmp4* expression in the ExE is reduced in size at 5.5 dpc, but is positioned correctly in relationship to the epiblast ($n = 6$) (Fig. 4B). However, in *Cripto*^{-/-}; *Cryptic*^{-/-} double mutants, *Bmp4*-positive cells are found lateral or distal to the epiblast, indicating a disrupted proximal-distal axis ($n = 3$) (Fig. 4C). Notably, a similar expression pattern is observed in *Nodal*^{-/-} mutants ($n = 4$) (Fig. 4D) as well as *Smad2*^{-/-} mutants (Waldrip et al., 1998). At 6.5 dpc, *Bmp4* expression is reduced or absent in the *Cripto*^{-/-}

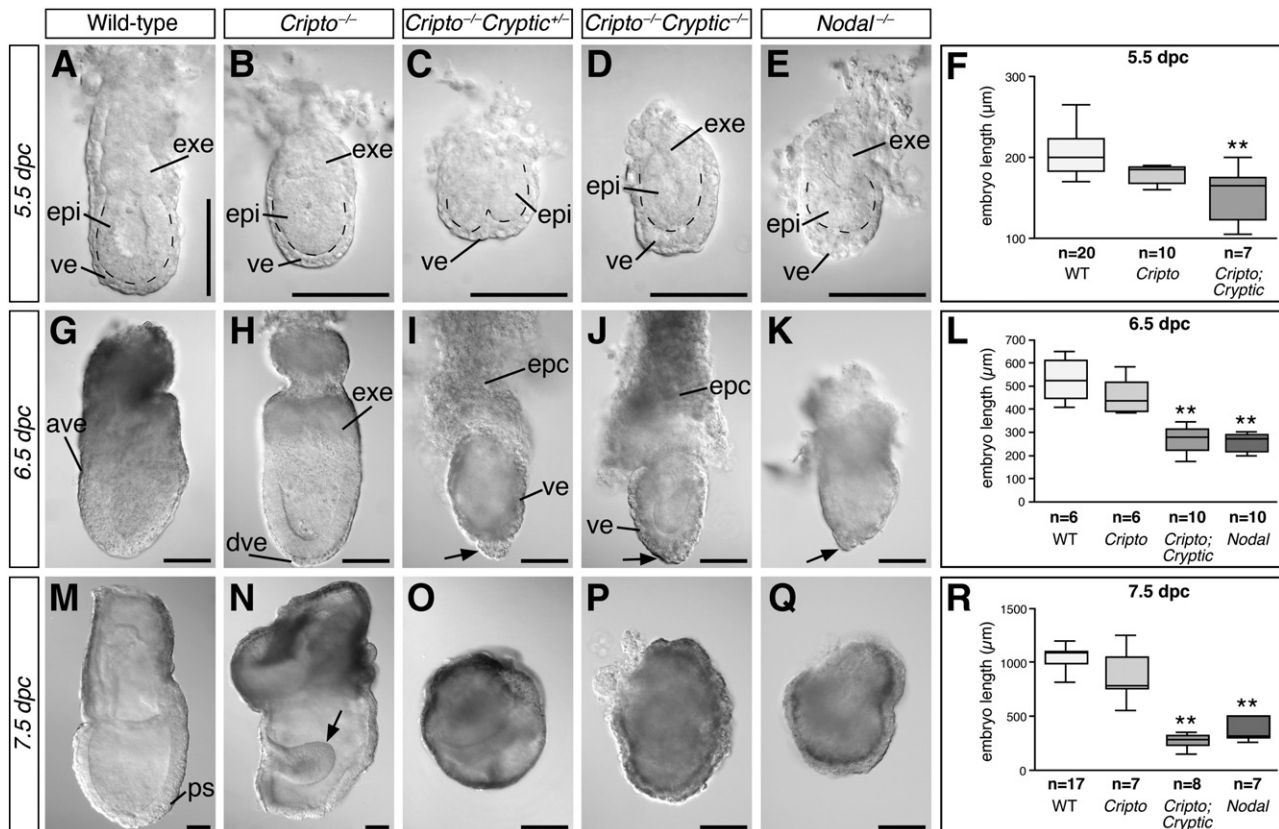


Fig. 2. Morphology and epiblast length of *Cripto*; *Cryptic* double mutants relative to wild-type, *Cripto*, and *Nodal* null mutants. (A–E) Embryos of the indicated genotypes at 5.5 dpc; dashed lines indicate boundary between epiblast and visceral endoderm. (G–K) Embryos of the indicated genotypes at 6.5 dpc; arrows in I–K indicate regions of thickened visceral endoderm. (M–Q) Embryos of the indicated genotypes at 7.5 dpc; arrow in N indicates expanded neuroectoderm that is typical of *Cripto*^{-/-} mutants (Ding et al., 1998). Scale bars correspond to 100 µm. (F, L, R) Box and whiskers plot of embryo length, measured from the base of the ectoplacental cone to the distal tip, in embryos of the indicated genotypes at 5.5, 6.5 and 7.5 dpc. Embryos of *Cripto*^{-/-}; *Cryptic*^{-/-} and *Cripto*^{-/-}; *Cryptic*^{+/-} genotypes are grouped together as *Cripto*; *Cryptic*. Abbreviations: ave, anterior visceral endoderm; epc, ectoplacental cone; epi, epiblast; exe, extraembryonic ectoderm; ps, primitive streak; ve, visceral endoderm.

Table 2
Genotypes of abnormal embryos from *Cripto*^{+/-}; *Cryptic*^{+/-} intercrosses.

Genotype	5.5 dpc ^a		6.5 dpc		7.5 dpc	
	Recovered	Expected	Recovered	Expected	Recovered	Expected
<i>Cripto</i> ^{-/-} ; <i>Cryptic</i> ^{+/+}	5	4.75	3	2.7	3	2.6
<i>Cripto</i> ^{-/-} ; <i>Cryptic</i> ^{+/-}	6 ^b	9.5	6 ^b	5.4	4 ^b	5.2
<i>Cripto</i> ^{-/-} ; <i>Cryptic</i> ^{-/-}	7	4.75	3	2.7	7	2.6
Other	58	57	31	32.2	28	31.5
Totals	76		43		42	

^a Data taken from Table 1.

^b Phenotype similar to that of *Cripto*^{-/-}; *Cryptic*^{-/-} mutants.

mutants ($n=3$; 2 lacked *Bmp4* expression, and 1 embryo displayed reduced but correctly positioned expression), and is completely absent in *Cripto*^{-/-}; *Cryptic*^{-/-} double mutants ($n=3$) (Figs. 4E–H). As is the case for *Bmp4*, expression of *Cdx2* in the distal ExE at 6.5 dpc (Beck et al., 1995) is reduced or absent in *Cripto*^{-/-} single mutants ($n=4$; 2 embryos lacked *Cdx2* expression, and 2 showed reduced but correctly patterned expression), and is completely lost in *Cripto*^{-/-}; *Cryptic*^{-/-} double mutants ($n=5$), similar to *Nodal*^{-/-} mutants ($n=2$) (Figs. 4I–L; data not shown).

Next, we examined the expression of *Mash2*, which marks differentiating trophoblast cells of the ectoplacental cone in wild-type embryos (Figs. 4M, P) (Guillemot et al., 1994). We found that the *Mash2* expression domain is greatly expanded into the ExE region in putative *Cripto*; *Cryptic* double mutants at 6.5 dpc ($n=2$) (Figs. 4O, R), in contrast with the relatively normal expression pattern in putative *Cripto* single mutants ($n=3$) (Figs. 4N, Q). (Note that embryo genotypes were deduced from their phenotypes in this experiment since the embryos were sectioned and not genotyped; thus, *Cripto*; *Cryptic* double mutants may correspond to either *Cripto*^{-/-}; *Cryptic*^{-/-} and *Cripto*^{-/-}; *Cryptic*^{+/-} genotypes.) Overall, these data on marker expression in the ExE are consistent with an inability to maintain the population of trophoblast stem cells, which instead differentiate towards an ectoplacental cone fate; a similar phenotype was previously reported for *Nodal* mutants (Guzman-Ayala et al., 2004).

EGF-CFC function in visceral endoderm

Finally, we examined the formation of the anterior visceral endoderm (AVE) in *Cripto*; *Cryptic* double mutants. First, we examined the expression of *Cerberus-like* (*Cer1*), which marks the AVE in wild-type embryos at 6.5 dpc, and found that expression was completely absent in *Cripto*^{-/-}; *Cryptic*^{-/-} double mutants ($n=2$) (Figs. 5A, D). Interestingly, we found that *Cripto*^{-/-} single mutants display heterogeneous *Cer1* expression, with some embryos expressing *Cer1* in the distal visceral endoderm ($n=2$), and others with no detectable *Cer1* expression ($n=3$) (Figs. 5B, C). Similarly, *Hex* expression also marks the AVE in wild-type embryos at 6.5 dpc (Fig. 5H) (Thomas et al., 1998), but is lost in *Cripto*^{-/-}; *Cryptic*^{-/-} double mutants ($n=4$), and displays expression in the distal visceral endoderm ($n=2$) or is completely absent ($n=4$) in *Cripto*^{-/-} single mutants (Figs. 5I–K).

Based on these findings, we further examined the visceral endoderm phenotype of *Cripto*; *Cryptic* double mutants as well as *Cripto*^{-/-} and *Cryptic*^{-/-} single mutants at 5.5 dpc. We found that expression of *Cer1* was not detectable in the distal visceral endoderm (DVE) of *Cripto*^{-/-} mutants ($n=5$), and was absent in *Cripto*^{-/-}; *Cryptic*^{-/-} double mutants ($n=2$) (Figs. 5E–G). However, expression of *alpha-fetoprotein* (*Afp*) remains present in the embryonic visceral endoderm of *Cripto*^{-/-} mutants at 5.5 dpc, although the expression in the extraembryonic visceral endoderm is lost ($n=2$) (Figs. 5L, M); in *Cripto*^{-/-}; *Cryptic*^{-/-} double mutants, *Afp* expression is completely

absent ($n=2$) (Fig. 5N). Furthermore, expression of the DVE marker *Lefty1* is also absent in *Cripto*^{-/-} mutants ($n=4$) as well as *Cripto*^{-/-}; *Cryptic*^{-/-} double mutants ($n=2$) (Figs. 5O, P, R), consistent with the previously reported absence of *Lefty1* expression in *Cripto*^{-/-} mutants at 6.5 dpc (Kimura et al., 2001). In contrast, *Lefty1* expression in the DVE appears normal in *Cryptic*^{-/-} single mutants (Fig. 5Q), as expected from their wild-type phenotype at early embryonic stages. Finally, *Lhx1* is broadly expressed in the embryonic visceral endoderm of wild-type embryos at 5.5 dpc (Perea-Gomez et al., 1999), yet its expression is absent in *Cripto*^{-/-} mutants ($n=3$) (Figs. 5S, T).

These findings indicate that specification of the DVE and more broadly the embryonic visceral endoderm requires EGF-CFC function prior to 5.5 dpc, consistent with a previously described role of Nodal in this process (Mesnard et al., 2006). Interestingly, there is a significant role for *Cripto* in this requirement for EGF-CFC function, even though *Cripto* is not expressed in the visceral endoderm. Furthermore, since *Cer1*, *Lefty1*, and *Lhx1* are believed to be directly or indirectly regulated by Nodal signaling, our results suggest that EGF-CFC genes are essential in specifying the DVE through the Nodal signaling pathway.

Discussion

Taken together, our analyses have demonstrated that partially redundant activities of the EGF-CFC genes *Cripto* and *Cryptic* play

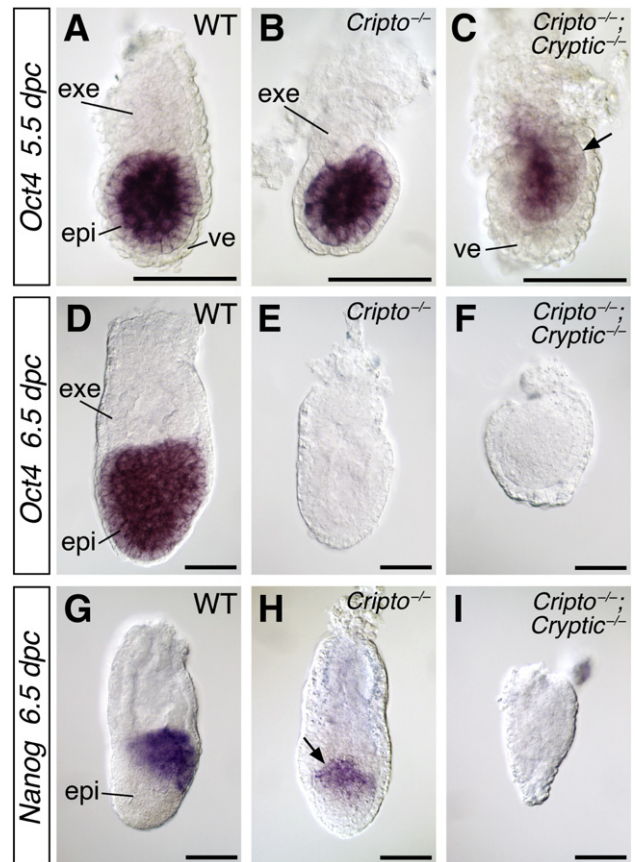


Fig. 3. Expression of epiblast markers in wild-type, *Cripto*, and *Cripto*; *Cryptic* mutants. (A–C) Expression of *Oct4* at 5.5 dpc; note the down-regulation in the *Cripto*^{-/-}; *Cryptic*^{-/-} double mutant (arrow). (D–F) *Oct4* is expressed at 6.5 dpc in the wild-type epiblast (D), but not in the *Cripto*^{-/-} or *Cripto*^{-/-}; *Cryptic*^{-/-} mutants (E, F). (G–I) Expression of *Nanog* at 6.5 dpc is down-regulated in the *Cripto*^{-/-} mutant, but is absent in the *Cripto*^{-/-}; *Cryptic*^{-/-} double mutant. *Nanog* expression is localized to the posterior epiblast in the wild-type embryo (G), but is proximally localized in the *Cripto*^{-/-} mutant (arrow in H), which lacks anterior–posterior polarity. Scale bars correspond to 100 μm. Abbreviations: epi, epiblast; exe, extraembryonic ectoderm; ve, visceral endoderm.

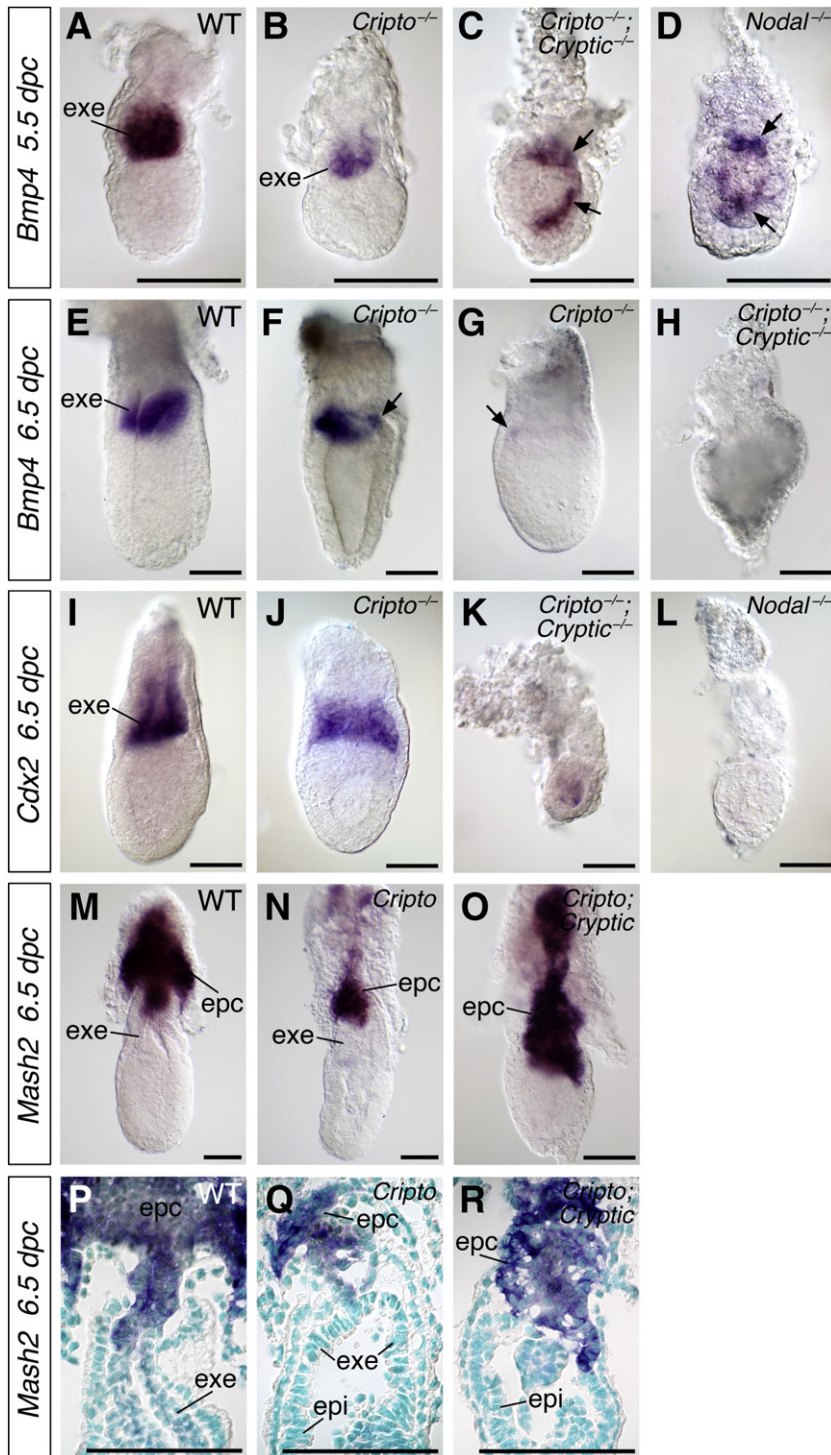


Fig. 4. Expression of extraembryonic ectoderm (ExE) and ectoplacental cone markers in wild-type, *Cripto*, and *Cripto; Cryptic* mutants. (A–D) *Bmp4* is expressed at 5.5 dpc in the ExE of wild-type (A), but is found only in the most distal part of the ExE in *Cripto*^{-/-} mutants (B). Expression of *Bmp4* is severely mislocalized in the presumptive epiblast (arrows) of *Cripto*^{-/-}; *Cryptic*^{-/-} double mutants (C) as well as *Nodal*^{-/-} mutants (D). (E–H) At 6.5 dpc, *Bmp4* is expressed in the distal ExE in wild-type (E), but is either reduced or nearly absent in *Cripto*^{-/-} single mutants (arrows in F, G), and is lost entirely in *Cripto*^{-/-}; *Cryptic*^{-/-} double mutants (H). (I–L) Expression of *Cdx2* at 6.5 dpc in the ExE in wild-type (I) is nearly normal in *Cripto*^{-/-} mutants (J), but is absent in both *Cripto*^{-/-}; *Cryptic*^{-/-} double mutants (K) and *Nodal*^{-/-} mutants (L). (M–O) Expression of *Mash2* in the ectoplacental cone of wild-type (M), putative *Cripto* mutant (N) and putative *Cripto; Cryptic* double mutant (O) embryos, showing an expanded domain of *Mash2* expression in the double mutant. (P–R) Longitudinal sections of the embryos shown in M–O, respectively; nuclei are counterstained with methyl green. In M–R, embryo genotypes were deduced from phenotypes, and the *Cripto; Cryptic* double mutant may correspond to either *Cripto*^{-/-}; *Cryptic*^{-/-} and *Cripto*^{-/-}; *Cryptic*^{+/-} genotypes. Scale bars correspond to 100 μm. Abbreviations: epc, ectoplacental cone; epi, epiblast; exe, extraembryonic ectoderm.

essential roles in patterning the early mouse embryo. Notably, the *Cripto; Cryptic* double mutant phenotype is highly similar to that for *Nodal* null mutants, indicating that EGF-CFC function is required for most or all *Nodal* signaling during early embryogenesis. As is the case

for *Nodal*, the combined functions of EGF-CFC genes are required for maintenance of the epiblast and ExE, as well as for formation of the DVE. However, the expression patterns of *Cripto* and *Cryptic* do not overlap in any of these tissues during pre-gastrulation development,

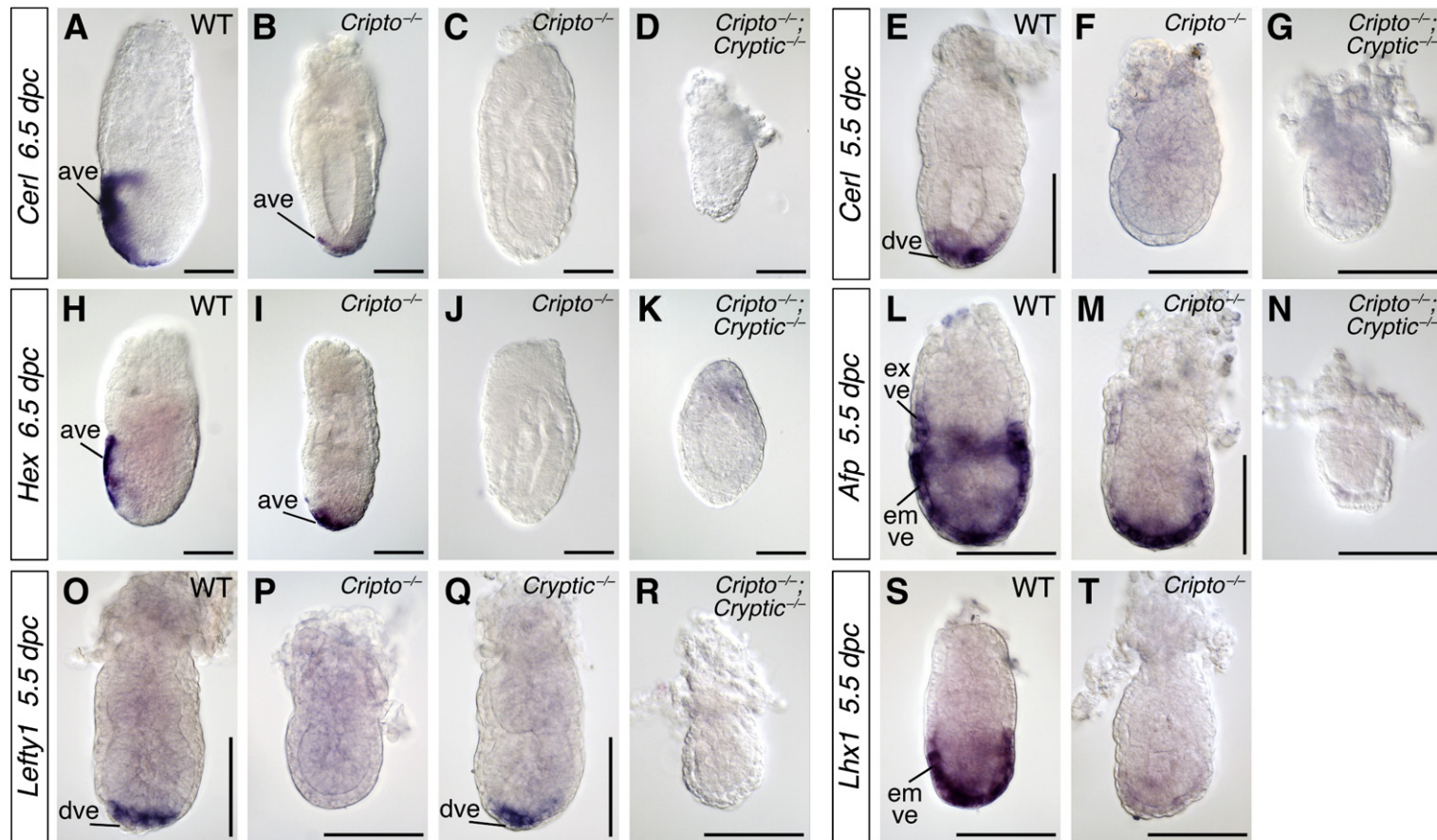


Fig. 5. Expression of visceral endoderm markers in wild-type, *Cripto*, *Cryptic*, and *Cripto; Cryptic* mutants. (A–D) At 6.5 dpc, *Cer1* is expressed in wild-type embryos in the anterior visceral endoderm (A), but is either mislocalized distally or absent in *Cripto*^{-/-} mutants (B, C), and is completely lost in *Cripto*^{-/-}; *Cryptic*^{-/-} double mutants (D). (E–G) At 5.5 dpc, *Cer1* is expressed in the distal visceral endoderm in wild-type embryos (E), but is absent in both *Cripto*^{-/-} mutants and *Cripto*^{-/-}; *Cryptic*^{-/-} double mutants (F, G). (H–K) Expression of *Hex* at 6.5 dpc is found in the wild-type anterior visceral endoderm (H), but is either mislocalized distally or is lost in *Cripto*^{-/-} mutants (I, J), and is absent in *Cripto*^{-/-}; *Cryptic*^{-/-} double mutants (K). (L–N) *Afp* (*alpha-fetoprotein*) is broadly expressed in the embryonic visceral endoderm (overlying the epiblast) and distal extraembryonic visceral endoderm (overlying the ExE) of wild-type embryos at 5.5 dpc (L), but is limited to the distal embryonic visceral endoderm in *Cripto*^{-/-} mutants (M) and is absent in *Cripto*^{-/-}; *Cryptic*^{-/-} double mutants (N). (O–R) *Lefty1* is expressed in the distal visceral endoderm at 5.5 dpc in wild-type as well *Cryptic*^{-/-} mutants (O, Q), but is absent in *Cripto*^{-/-} mutants and *Cripto*^{-/-}; *Cryptic*^{-/-} double mutants (P, R). (S, T) *Lhx1* is expressed in the wild-type embryonic visceral endoderm at 5.5 dpc (S), but is absent in *Cripto*^{-/-} mutants (T). Scale bars correspond to 100 μ m. Abbreviations: ave, anterior visceral endoderm; dve, distal visceral endoderm; emve, embryonic visceral endoderm; exve, extraembryonic visceral endoderm.

indicating that their redundant activities are a consequence of non-cell-autonomous function.

Non-autonomous EGF-CFC function

The existence of two EGF-CFC genes in mammalian genomes and only one gene (*oep*) in zebrafish suggests that *Cripto* and *Cryptic* originated from a common ancestor and subsequently acquired functional divergency. However, our studies have shown that these two EGF-CFC genes retain common redundant functions, and that in the absence of *Cripto*, *Cryptic* is haploinsufficient. In addition, we have observed a defect in maintenance of pluripotent marker expression in *Cripto* null mutants alone, consistent with the previously described premature neural differentiation of epiblast (Ding et al., 1998; Kimura et al., 2001; Liguori et al., 2003); a similar phenotype has been described for *Nodal* mutants (Camus et al., 2006; Lu and Robertson, 2004; Mesnard et al., 2006).

Previous studies have shown that *Cripto* mutants form a partially functional DVE that fails to translocate, based on the expression of *Hex* and *Cer1* in the distally mispositioned AVE at 6.75 dpc (Ding et al., 1998). In the present work, we observe that this mispositioning of *Hex* and *Cer1* expression in the distal visceral endoderm is heterogeneous in *Cripto* mutants, with some embryos lacking expression altogether; similar heterogeneity was found for marker expression in the epiblast and ExE. This phenotypic heterogeneity may be due to a different strain background from our previous study, since the *Cripto* mutant mice have now been backcrossed extensively against C57BL/6 in our laboratory. In addition, our data suggest that expression of *Cer1* may be developmentally delayed in *Cripto* mutants, since it was not detected at 5.5 dpc. Thus, the failure of DVE movement in *Cripto* mutants may be due at least in part to the absence of *Lefty1* and *Cer1*

expression at 5.5 dpc, which are believed to drive DVE movement (Yamamoto et al., 2004). However, the ability of *Cripto* mutants to form a partial DVE is likely to result from the activity of *Cryptic* expressed in the proximal visceral endoderm.

The lack of overlapping expression for *Cripto* and *Cryptic* is particularly striking given the multiple phenotypes of *Cripto*; *Cryptic* double mutants that are not observed in the individual single mutants. Thus, the ability of *Cryptic* expressed in the visceral endoderm to promote formation of a DVE (albeit defective) in *Cripto* mutants presumably reflects a cell-autonomous activity of *Cryptic*. In contrast, the ability of *Cripto* expressed in the epiblast to promote normal AVE formation and movement in *Cryptic* mutants would be non-cell-autonomous. Moreover, the ability of *Cryptic* to promote epiblast maintenance in the absence of *Cripto* is presumably non-cell-autonomous, since *Cryptic* is only expressed in the visceral endoderm. Finally, neither *Cripto* nor *Cryptic* are expressed in the ExE, yet these two genes are required for maintenance of undifferentiated ExE. The simplest explanation for these observations is that both *Cripto* and *Cryptic* act non-cell-autonomously during early embryogenesis, as previously shown for *Cripto* in axial mesendoderm formation during gastrulation (Chu et al., 2005), and more generally in embryonic development (Xu et al., 1999). Thus, we propose that *Cripto* and/or *Cryptic* act non-cell-autonomously in distinct contexts in epiblast maintenance, ExE maintenance, and AVE formation and movement (Fig. 6).

In principle, these non-cell-autonomous functions of *Cripto* and *Cryptic* could reflect direct or indirect mechanisms. In the former situation, EGF-CFC proteins could be released from cells of one tissue and act in a paracrine manner on cells of a neighboring tissue. In the latter case, downstream targets of *Cripto* or *Cryptic* could mediate the relevant intercellular interactions. In the case of *Cripto*, our genetic

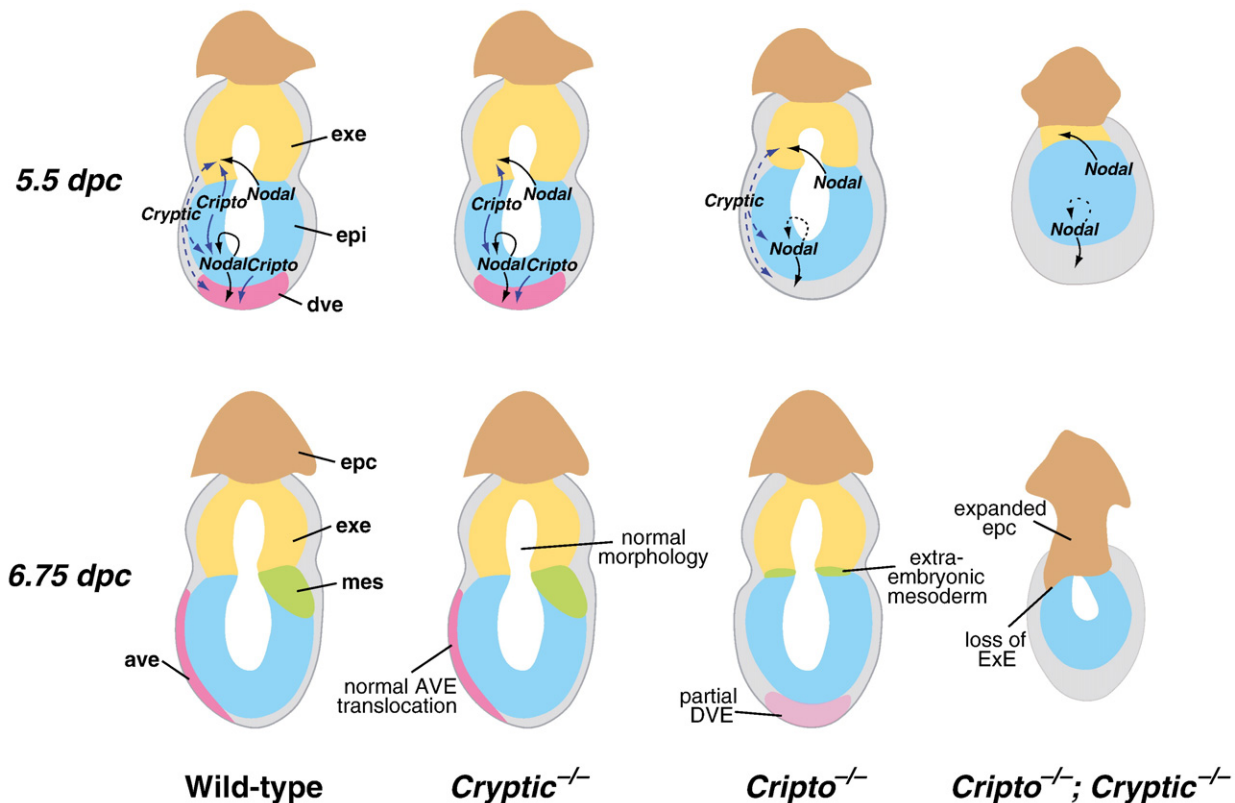


Fig. 6. Model for non-autonomous redundant functions of *Cripto* and *Cryptic*. Schematic diagrams of the phenotype of wild-type, *Cryptic* null mutant, *Cripto* null mutant, and *Cripto*; *Cryptic* double mutant embryos at 5.5 and 6.75 dpc. Suggested pathways of *Nodal* and EGF-CFC activity are shown (arrows). Note that the proposed signaling interactions shown at 5.5 dpc could in principle occur at earlier stages, and that the arrows may correspond to direct or indirect signaling events. Abbreviations: ave, anterior visceral endoderm; dve, distal visceral endoderm; epc, ectoplacental cone; epi, epiblast; exe, extraembryonic ectoderm; mes, mesoderm.

analyses have previously suggested that the non-cell-autonomous function of *Cripto* in axial mesendoderm reflects a direct, *trans*-acting activity of *Cripto* protein, thus favoring the first model (Chu et al., 2005). However, it remains unclear whether the roles of EGF-CFC proteins in visceral endoderm and the ExE are direct or indirect, particularly since their temporal requirements during embryogenesis are also unknown. Perhaps consistent with a direct role, *Lefty1* is expressed normally in the DVE of *Cryptic* null mutants at 5.5 dpc (Fig. 5Q), which is notable since the relevant *Lefty1* promoter element contains essential FoxH1 binding sites, indicating that it is responsive to Nodal signaling (Takaoka et al., 2006). Also favoring a direct role for EGF-CFC proteins, weak phospho-Smad2 immunoreactivity can be detected in the ExE at 5.5 dpc, and is abolished by culture in the presence of the ALK4/ALK5/ALK7 inhibitor SB431542 (Yamamoto et al., 2009). On the other hand, this phospho-Smad2 immunoreactivity may be due to a different TGF β signaling factor that does not require EGF-CFC activity, such as Activin. Indeed, a recent study has suggested that Activin, but not Nodal, is required for ExE as well as trophoblast stem cell maintenance, and that the ExE requirement for Nodal (and presumably EGF-CFC) function may reflect an autoregulatory loop for epiblast expression of FGF4, which in turn acts as a paracrine signal to the ExE (Natale et al., 2009).

Although EGF-CFC proteins were originally identified as strictly *cis*-acting co-receptors for Nodal ligands that act cell-autonomously in zebrafish (Gritsman et al., 1999; Schier et al., 1997; Strahle et al., 1997), there is considerable evidence for their *trans*-acting functions in cell culture and *in vivo* (Chu et al., 2005; Minchiotti et al., 2001; Parisi et al., 2003; Yan et al., 2002). For example, overexpression of a truncated form of zebrafish *Oep* that lacks the C-terminal GPI anchor in the extraembryonic yolk syncytial layer can rescue the embryonic defects of *oep* mutants, indicating non-autonomous function (Gritsman et al., 1999; Minchiotti et al., 2001). In principle, such paracrine responses to *Cripto* can be due to activation of the Nodal pathway, or can be Nodal-independent in other contexts (Bianco et al., 2002; Bianco et al., 2003). *Cripto* can be released from the cell membrane after cleavage of its GPI-linkage by GPI-phospholipase D (Minchiotti et al., 2000; Watanabe et al., 2007), while activity of human *Cryptic* is modulated by a C-terminal hydrophilic extension that can lead to formation of both GPI-linked and soluble forms of the protein (Watanabe et al., 2008). However, the resulting soluble EGF-CFC proteins may be less efficient at signaling since they compete for Nodal binding with secreted inhibitors (Blanchet et al., 2008; Constam, 2009). Thus, paracrine activity of *Cripto* and *Cryptic* may be tightly regulated by *Cerl* as well as *Lefty*; notably, *Lefty* proteins can also interact directly with EGF-CFC proteins (Chen and Shen, 2004; Cheng et al., 2004).

Partial functional redundancy of EGF-CFC genes in mediating Nodal signaling

Our findings demonstrate the strong similarity of the *Cripto*; *Cryptic* double mutant phenotype to the *Nodal* null phenotype. These *Nodal* mutant phenotypes include the defective maintenance of the extraembryonic ectoderm (Brennan et al., 2001; Guzman-Ayala et al., 2004), as well as the precocious neural differentiation of epiblast (Camus et al., 2006), which is related to a requirement for epiblast proliferation and size control *in vivo* (Mesnard et al., 2006). Furthermore, Nodal signaling is required for maintenance of undifferentiated human ES cells and mouse epiblast stem cells (Brons et al., 2007; James et al., 2005; Tesar et al., 2007), most likely through up-regulation of *Nanog* expression (Vallier et al., 2009; Xu et al., 2008). In each case, the *Nodal* mutant phenotype is highly similar to the *Cripto*; *Cryptic* double mutant phenotype, supporting the conclusion that EGF-CFC proteins mediate all aspects of Nodal signaling *in vivo*.

Our results are relevant for previous studies that have addressed whether Nodal signaling always requires EGF-CFC function. For example, one recent study showed that purified Nodal precursor

protein can act on ExE explants, which lack EGF-CFC expression, suggesting that Nodal precursor signals from the epiblast to the ExE in an EGF-CFC independent manner (Ben-Haim et al., 2006). However, an alternative explanation for this observation is that these ExE explants may have already been “primed” for Nodal responsiveness by paracrine *Cripto* and *Cryptic* by 5.5 dpc, and might not require EGF-CFC activity thereafter. Furthermore, our results can also account for the *Cripto*-independent Nodal signaling that was deduced from the ability of a *Cerl* null mutant to partially suppress the *Cripto* mutant phenotype (Liguori et al., 2008). In this case, we propose that the removal of a Nodal antagonist in *Cripto*; *Cerl* double mutants may result in greater range and/or activity of Nodal protein and possibly of *trans*-acting *Cryptic* protein as well. Thus, in the absence of *Cerl*, Nodal could mediate *Cryptic*-dependent rescue of the *Cripto* mutant phenotype.

Although *Cripto* and *Cryptic* display functional redundancy, our findings suggest that their activities are not wholly equivalent. The embryonic lethality of *Cripto* null mutants suggests that *Cripto* is more essential than *Cryptic*, and therefore that *Cripto* may be more important than *Cryptic* in mediating Nodal function, a conclusion that is also consistent with the observed haploinsufficiency of *Cryptic* in the absence of *Cripto* function. This difference between *Cripto* and *Cryptic* may simply be due to relative differences in expression levels, or the expression of *Cripto* in the epiblast, where the requirement for mediating Nodal activity is greatest. Alternatively, this difference may reflect a mechanistic distinction between *Cripto* and *Cryptic* with respect to their non-autonomous activities.

Our findings are also relevant for assessing whether EGF-CFC proteins may have activities that are independent of Nodal in early embryogenesis. In particular, recent work has shown that EGF-CFC proteins can mediate signaling by additional TGF β ligands during early vertebrate embryogenesis (Chen et al., 2006; Cheng et al., 2003). One of these TGF β ligands, GDF3 (Growth-Differentiation Factor-3), has a Nodal-like activity in *Xenopus* embryos as well as EGF-CFC-dependent signaling activity in cell culture, while *Gdf3* null mutants display phenotypes resembling those of *Nodal* hypomorphs (Andersson et al., 2007, 2008; Chen et al., 2006); however, we note that other studies in *Xenopus* embryos have concluded that GDF3 primarily acts as a BMP inhibitor *in vivo* (Levine and Brivanlou, 2006; Levine et al., 2009). Furthermore, the TGF β ligand GDF1 also stimulates Nodal pathway activity in an EGF-CFC-dependent manner (Andersson et al., 2006; Cheng et al., 2003), and can heterodimerize with Nodal to potentiate Nodal activity, possibly by increasing long-range signaling (Tanaka et al., 2007).

Finally, it remains conceivable that EGF-CFC proteins may have activities that are entirely independent of the TGF β /Activin/Nodal pathway. For example, previous work has suggested a Nodal-independent pathway that involves interaction of *Cripto* with glypican-1 and subsequent activation of c-Src in mammary epithelial cells (Bianco et al., 2003), while a recent study has shown that *Cripto* can facilitate signaling through Notch receptors in embryonal carcinoma cells (Watanabe et al., 2009). In addition, *Cripto* and the *Xenopus* EGF-CFC protein FRL-1 have been proposed to mediate signaling by Wnt11 through the canonical Wnt/ β -catenin signaling pathway (Tao et al., 2005). Notably, the analysis of a *Cripto* hypomorphic allele containing a point mutation that eliminates activity in cell culture assays for Nodal function has suggested that many of the *in vivo* functions of *Cripto* are due to Nodal pathway-independent activities (D'Andrea et al., 2008). However, given the overall similarity of the *Cripto*; *Cryptic* double mutant phenotype with that of *Nodal* null mutants, if such Nodal pathway-independent activities of EGF-CFC proteins occur during early embryogenesis, they should be largely redundant with Nodal pathway activity. Of course, these data do not exclude the possibility that EGF-CFC proteins may have Nodal pathway-independent activities at later stages of development, or in cancer or other disease processes. Investigation of such Nodal-independent EGF-CFC functions will be of continuing interest in future studies.

Acknowledgments

We are grateful to Jixiang Ding for his initial observations on the *Cripto*; *Cryptic* double mutant phenotype. We thank Richard Behringer, Eddy De Robertis, Hiroshi Hamada, Brigid Hogan, Liz Robertson, Janet Rossant, and Austin Smith for reagents, and Antonella Galli, Marianna Kruthof-de Julio, and David-Emlyn Parfitt for comments on the manuscript. This work was supported by NIH grant HD42837 (M.M.S.).

References

- Andersson, O., Reissmann, E., Jornvall, H., Ibanez, C.F., 2006. Synergistic interaction between Gdf1 and Nodal during anterior axis development. *Dev. Biol.* 293, 370–381.
- Andersson, O., Bertolino, P., Ibanez, C.F., 2007. Distinct and cooperative roles of mammalian Vg1 homologs GDF1 and GDF3 during early embryonic development. *Dev. Biol.* 311, 500–511.
- Andersson, O., Korach-Andre, M., Reissmann, E., Ibanez, C.F., Bertolino, P., 2008. Growth/differentiation factor 3 signals through ALK7 and regulates accumulation of adipose tissue and diet-induced obesity. *Proc. Natl. Acad. Sci. U.S.A.* 105, 7252–7256.
- Beck, F., Erler, T., Russell, A., James, R., 1995. Expression of Cdx-2 in the mouse embryo and placenta: possible role in patterning of the extra-embryonic membranes. *Dev. Dyn.* 204, 219–227.
- Belo, J.A., Bouwmeester, T., Leyns, L., Kertesz, N., Gallo, M., Follettie, M., De Robertis, E.M., 1997. Cerberus-like is a secreted factor with neutralizing activity expressed in the anterior primitive endoderm of the mouse gastrula. *Mech. Dev.* 68, 45–57.
- Ben-Haim, N., Lu, C., Guzman-Ayala, M., Pescatore, L., Mesnard, D., Bischofberger, M., Naef, F., Robertson, E.J., Constam, D.B., 2006. The Nodal precursor acting via activin receptors induces mesoderm by maintaining a source of its convertases and BMP4. *Dev. Cell* 11, 313–323.
- Bianco, C., Adkins, H.B., Wechselberger, C., Seno, M., Normanno, N., De Luca, A., Sun, Y., Khan, N., Kenney, N., Ebert, A., Williams, K.P., Sanicola, M., Salomon, D.S., 2002. *Cripto-1* activates Nodal- and ALK4-dependent and -independent signaling pathways in mammary epithelial cells. *Mol. Cell. Biol.* 22, 2586–2597.
- Bianco, C., Strizzi, L., Rehman, A., Normanno, N., Wechselberger, C., Sun, Y., Khan, N., Hirota, M., Adkins, H., Williams, K., Margolis, R.U., Sanicola, M., Salomon, D.S., 2003. A Nodal- and ALK4-independent signaling pathway activated by *Cripto-1* through Glypican-1 and c-Src. *Cancer Res.* 63, 1192–1197.
- Blanchet, M.H., Le Good, J.A., Oorschot, V., Baflost, S., Minchiotti, G., Klumperman, J., Constam, D.B., 2008. *Cripto* localizes Nodal at the limiting membrane of early endosomes. *Sci. Signal.* 1, ra13.
- Brennan, J., Lu, C.C., Norris, D.P., Rodriguez, T.A., Beddington, R.S., Robertson, E.J., 2001. Nodal signalling in the epiblast patterns the early mouse embryo. *Nature* 411, 965–969.
- Brons, I.G., Smithers, L.E., Trotter, M.W., Rugg-Gunn, P., Sun, B., Chuva de Sousa Lopes, S.M., Howlett, S.K., Clarkson, A., Ahrlund-Richter, L., Pedersen, R.A., Vallier, L., 2007. Derivation of pluripotent epiblast stem cells from mammalian embryos. *Nature* 448, 191–195.
- Camus, A., Perea-Gomez, A., Moreau, A., Collignon, J., 2006. Absence of Nodal signaling promotes precocious neural differentiation in the mouse embryo. *Dev. Biol.* 295, 743–755.
- Chambers, I., Colby, D., Robertson, M., Nichols, J., Lee, S., Tweedie, S., Smith, A., 2003. Functional expression cloning of Nanog, a pluripotency sustaining factor in embryonic stem cells. *Cell* 113, 643–655.
- Chen, C., Shen, M.M., 2004. Two modes by which Lefty proteins inhibit Nodal signaling. *Curr. Biol.* 14, 618–624.
- Chen, X., Rubock, M.J., Whitman, M., 1996. A transcriptional partner for MAD proteins in TGF-beta signalling. *Nature* 383, 691–696.
- Chen, X., Weisberg, E., Fridmacher, V., Watanabe, M., Naco, G., Whitman, M., 1997. Smad4 and FAST-1 in the assembly of activin-responsive factor. *Nature* 389, 85–89.
- Chen, C., Ware, S.M., Sato, A., Houston-Hawkins, D.E., Habas, R., Matzuk, M.M., Shen, M.M., Brown, C.W., 2006. The Vg1-related protein Gdf3 acts in a Nodal signaling pathway in the pre-gastrulation mouse embryo. *Development* 133, 319–329.
- Cheng, S.K., Olale, F., Bennett, J.T., Brivanlou, A.H., Schier, A.F., 2003. EGF-CFC proteins are essential coreceptors for the TGF-beta signals Vg1 and GDF1. *Genes Dev.* 17, 31–36.
- Cheng, S.K., Olale, F., Brivanlou, A.H., Schier, A.F., 2004. Lefty blocks a subset of TGFbeta signals by antagonizing EGF-CFC coreceptors. *PLoS Biol.* 2, 215–226.
- Chu, J., Ding, J., Jeays-Ward, K., Price, S.M., Placzek, M., Shen, M.M., 2005. Non-cell-autonomous role for *Cripto* in axial midline formation during vertebrate embryogenesis. *Development* 132, 5539–5551.
- Collignon, J., Varlet, I., Robertson, E.J., 1996. Relationship between asymmetric *nodal* expression and the direction of embryonic turning. *Nature* 381, 155–158.
- Constam, D.B., 2009. Running the gauntlet: an overview of the modalities of travel employed by the putative morphogen Nodal. *Curr. Opin. Genet. Dev.* 302–307.
- Coucouvanis, E., Martin, G.R., 1999. BMP signaling plays a role in visceral endoderm differentiation and cavitation in the early mouse embryo. *Development* 126, 535–546.
- D'Andrea, D., Liguori, G.L., Le Good, J.A., Lonardo, E., Andersson, O., Constam, D.B., Persico, M.G., Minchiotti, G., 2008. *Cripto* promotes A-P axis specification independently of its stimulatory effect on Nodal autoinduction. *J. Cell Biol.* 180, 597–605.
- Ding, J., Yang, L., Yan, Y.T., Chen, A., Desai, N., Wynshaw-Boris, A., Shen, M.M., 1998. *Cripto* is required for correct orientation of the anterior–posterior axis in the mouse embryo. *Nature* 395, 702–707.
- Gaio, U., Schweickert, A., Fischer, A.N., Muller, T., Ozelik, C., Lankes, W., Strehle, M., Britsch, S., Blum, M., Birchmeier, C., 1999. A role of the *cryptic* gene in the correct establishment of the left–right axis. *Curr. Biol.* 9, 1339–1342.
- Germain, S., Howell, M., Esslemont, G.M., Hill, C.S., 2000. Homeodomain and winged-helix transcription factors recruit activated Smads to distinct promoter elements via a common Smad interaction motif. *Genes Dev.* 14, 435–451.
- Gritsman, K., Zhang, J., Cheng, S., Heckscher, E., Talbot, W.S., Schier, A.F., 1999. The EGF-CFC protein one-eyed pinhead is essential for Nodal signaling. *Cell* 97, 121–132.
- Guillemot, F., Nagy, A., Auerbach, A., Rossant, J., Joyner, A.L., 1994. Essential role of *Mash-2* in extraembryonic development. *Nature* 371, 333–336.
- Guzman-Ayala, M., Ben-Haim, N., Beck, S., Constam, D.B., 2004. Nodal protein processing and fibroblast growth factor 4 synergize to maintain a trophoblast stem cell microenvironment. *Proc. Natl. Acad. Sci. U.S.A.* 101, 15656–15660.
- James, D., Levine, A.J., Besser, D., Hemmati-Brivanlou, A., 2005. TGFbeta/activin/nodal signaling is necessary for the maintenance of pluripotency in human embryonic stem cells. *Development* 132, 1273–1282.
- Kimura, C., Shen, M.M., Takeda, N., Aizawa, S., Matsuo, I., 2001. Complementary functions of *Otx2* and *Cripto* in initial patterning of mouse epiblast. *Dev. Biol.* 235, 12–32.
- Kumar, A., Novoselov, V., Celeste, A.J., Wolfman, N.M., ten Dijke, P., Kuehn, M.R., 2001. Nodal signaling uses activin and transforming growth factor-beta receptor-regulated Smads. *J. Biol. Chem.* 276, 656–661.
- Levine, A.J., Brivanlou, A.H., 2006. GDF3, a BMP inhibitor, regulates cell fate in stem cells and early embryos. *Development* 133, 209–216.
- Levine, A.J., Levine, Z.J., Brivanlou, A.H., 2009. GDF3 is a BMP inhibitor that can activate Nodal signaling only at very high doses. *Dev. Biol.* 325, 43–48.
- Liguori, G.L., Echevarria, D., Improta, R., Signore, M., Adamson, E., Martinez, S., Persico, M.G., 2003. Anterior neural plate regionalization in *cripto* null mutant mouse embryos in the absence of node and primitive streak. *Dev. Biol.* 264, 537–549.
- Liguori, G.L., Borges, A.C., D'Andrea, D., Liguori, A., Goncalves, L., Salgueiro, A.M., Persico, M.G., Belo, J.A., 2008. *Cripto*-independent Nodal signaling promotes positioning of the A–P axis in the early mouse embryo. *Dev. Biol.* 315, 280–289.
- Lu, C.C., Robertson, E.J., 2004. Multiple roles for Nodal in the epiblast of the mouse embryo in the establishment of anterior–posterior patterning. *Dev. Biol.* 273, 149–159.
- Meno, C., Ito, Y., Saijoh, Y., Matsuda, Y., Tashiro, K., Kuhara, S., Hamada, H., 1997. Two closely-related left–right asymmetrically expressed genes, *lefty-1* and *lefty-2*: their distinct expression domains, chromosomal linkage and direct neutralizing activity in *Xenopus* embryos. *Genes Cells* 2, 513–524.
- Mesnard, D., Guzman-Ayala, M., Constam, D.B., 2006. Nodal specifies embryonic visceral endoderm and sustains pluripotent cells in the epiblast before overt axial patterning. *Development* 133, 2497–2505.
- Minchiotti, G., Parisi, S., Liguori, G., Signore, M., Lania, G., Adamson, E.D., Lago, C.T., Persico, M.G., 2000. Membrane-anchorage of *Cripto* protein by glycosylphosphatidylinositol and its distribution during early mouse development. *Mech. Dev.* 90, 133–142.
- Minchiotti, G., Manco, G., Parisi, S., Lago, C.T., Rosa, F., Persico, M.G., 2001. Structure–function analysis of the EGF-CFC family member *Cripto* identifies residues essential for nodal signalling. *Development* 128, 4501–4510.
- Morkel, M., Huelsken, J., Wakamiya, M., Ding, J., van de Wetering, M., Clevers, H., Taketo, M.M., Behringer, R.R., Shen, M.M., Birchmeier, W., 2003. Beta-catenin regulates *Cripto*- and *Wnt3*-dependent gene expression programs in mouse axis and mesoderm formation. *Development* 130, 6283–6294.
- Natale, D.R., Hemberger, M., Hughes, M., Cross, J.C., 2009. Activin promotes differentiation of cultured mouse trophoblast stem cells towards a labyrinth cell fate. *Dev. Biol.* 335, 120–131.
- Norris, D.P., Robertson, E.J., 1999. Asymmetric and node-specific *nodal* expression patterns are controlled by two distinct cis-acting regulatory elements. *Genes Dev.* 13, 1575–1588.
- Parisi, S., D'Andrea, D., Lago, C.T., Adamson, E.D., Persico, M.G., Minchiotti, G., 2003. Nodal-dependent *Cripto* signaling promotes cardiomyogenesis and redirects the neural fate of embryonic stem cells. *J. Cell Biol.* 163, 303–314.
- Perea-Gomez, A., Shawlot, W., Sasaki, H., Behringer, R.R., Ang, S., 1999. HNF3beta and *Lim1* interact in the visceral endoderm to regulate primitive streak formation and anterior–posterior polarity in the mouse embryo. *Development* 126, 4499–4511.
- Reissmann, E., Jornvall, H., Blokzijl, A., Andersson, O., Chang, C., Minchiotti, G., Persico, M.G., Ibanez, C.F., Brivanlou, A.H., 2001. The orphan receptor ALK7 and the Activin receptor ALK4 mediate signaling by Nodal proteins during vertebrate development. *Genes Dev.* 15, 2010–2022.
- Rosner, M.H., Vigano, M.A., Ozato, K., Timmons, P.M., Poirier, F., Rigby, P.W.J., Staudt, L.M., 1990. A POU-domain transcription factor in early stem cells and germ cells of the mammalian embryo. *Nature* 345, 686–692.
- Schier, A.F., 2003. Nodal signaling in vertebrate development. *Annu. Rev. Cell Dev. Biol.* 19, 589–621.
- Schier, A.F., Shen, M.M., 2000. Nodal signalling in vertebrate development. *Nature* 403, 385–389.
- Schier, A.F., Neuhaus, S.C.F., Helde, K.A., Talbot, W.S., Driever, W., 1997. The *one-eyed pinhead* gene functions in mesoderm and endoderm formation in zebrafish and interacts with *no tail*. *Development* 124, 327–342.
- Shawlot, W., Behringer, R.R., 1995. Requirement for *Lim1* in head-organizer function. *Nature* 374, 425–430.
- Shen, M.M., 2007. Nodal signaling: developmental roles and regulation. *Development* 134, 1023–1034.
- Shen, M.M., Schier, A.F., 2000. The *EGF-CFC* gene family in vertebrate development. *Trends Genet.* 16, 303–309.

- Shen, M.M., Wang, H., Leder, P., 1997. A differential display strategy identifies *Cryptic*, a novel EGF-related gene expressed in the axial and lateral mesoderm during mouse gastrulation. *Development* 124, 429–442.
- Strahle, U., Jesuthasan, S., Blader, P., Garcia-Villalba, P., Hatta, K., Ingham, P.W., 1997. One-eyed pinhead is required for development of the ventral midline of the zebrafish (*Danio rerio*) neural tube. *Genes Funct.* 1, 131–148.
- Strumpf, D., Mao, C.A., Yamanaka, Y., Ralston, A., Chawengsaksophak, K., Beck, F., Rossant, J., 2005. *Cdx2* is required for correct cell fate specification and differentiation of trophoblast in the mouse blastocyst. *Development* 132, 2093–2102.
- Takaoka, K., Yamamoto, M., Shiratori, H., Meno, C., Rossant, J., Saijoh, Y., Hamada, H., 2006. The mouse embryo autonomously acquires anterior–posterior polarity at implantation. *Dev. Cell* 10, 451–459.
- Tanaka, C., Sakuma, R., Nakamura, T., Hamada, H., Saijoh, Y., 2007. Long-range action of Nodal requires interaction with GDF1. *Genes Dev.* 21, 3272–3282.
- Tao, Q., Yokota, C., Puck, H., Kofron, M., Birsoy, B., Yan, D., Asashima, M., Wylie, C.C., Lin, X., Heasman, J., 2005. Maternal *Wnt11* activates the canonical *Wnt* signaling pathway required for axis formation in *Xenopus* embryos. *Cell* 120, 857–871.
- Tesar, P.J., Chenoweth, J.G., Brook, F.A., Davies, T.J., Evans, E.P., Mack, D.L., Gardner, R.L., McKay, R.D., 2007. New cell lines from mouse epiblast share defining features with human embryonic stem cells. *Nature* 448, 196–199.
- Thomas, P.Q., Brown, A., Beddington, R.S.P., 1998. *Hex*: a homeobox gene revealing peri-implantation asymmetry in the mouse embryo and an early transient marker of endothelial cell precursors. *Development* 125, 85–94.
- Tilghman, S.M., Kioussis, D., Gorin, M.B., Ruiz, J.P., Ingram, R.S., 1979. The presence of intervening sequences in the alpha-fetoprotein gene of the mouse. *J. Biol. Chem.* 254, 7393–7399.
- Vallier, L., Mendjan, S., Brown, S., Chng, Z., Teo, A., Smithers, L.E., Trotter, M.W., Cho, C.H., Martinez, A., Rugg-Gunn, P., Brons, G., Pedersen, R.A., 2009. Activin/Nodal signalling maintains pluripotency by controlling *Nanog* expression. *Development* 136, 1339–1349.
- Waldrup, W.R., Bikoff, E.K., Hoodless, P.A., Wrana, J.L., Robertson, E.J., 1998. *Smad2* signaling in extraembryonic tissues determines anterior–posterior polarity of the early mouse embryo. *Cell* 92, 797–808.
- Watanabe, K., Bianco, C., Strizzi, L., Hamada, S., Mancino, M., Bailly, V., Mo, W., Wen, D., Miatkowski, K., Gonzales, M., Sanicola, M., Seno, M., Salomon, D.S., 2007. Growth factor induction of *Cripto-1* shedding by glycosylphosphatidylinositol-phospholipase D and enhancement of endothelial cell migration. *J. Biol. Chem.* 282, 31643–31655.
- Watanabe, K., Nagaoka, T., Strizzi, L., Mancino, M., Gonzales, M., Bianco, C., Salomon, D.S., 2008. Characterization of the glycosylphosphatidylinositol-anchor signal sequence of human *Cryptic* with a hydrophilic extension. *Biochim. Biophys. Acta* 1778, 2671–2681.
- Watanabe, K., Nagaoka, T., Lee, J.M., Bianco, C., Gonzales, M., Castro, N.P., Rangel, M.C., Sakamoto, K., Sun, Y., Callahan, R., Salomon, D.S., 2009. Enhancement of Notch receptor maturation and signaling sensitivity by *Cripto-1*. *J. Cell Biol.* 187, 343–353.
- Wechselberger, C., Bianco, C., Strizzi, L., Ebert, A.D., Kenney, N., Sun, Y., Salomon, D.S., 2005. Modulation of TGF-beta signaling by EGF-CFC proteins. *Exp. Cell Res.* 310, 249–255.
- Whitman, M., 2001. Nodal signaling in early vertebrate embryos. Themes and variations. *Dev. Cell* 1, 605–617.
- Winnier, G., Blessing, M., Labosky, P.A., Hogan, B.L., 1995. Bone morphogenetic protein-4 is required for mesoderm formation and patterning in the mouse. *Genes Dev.* 9, 2105–2116.
- Xu, C., Liguori, G., Persico, M.G., Adamson, E.D., 1999. Abrogation of the *Cripto* gene in mouse leads to failure of postgastrulation morphogenesis and lack of differentiation of cardiomyocytes. *Development* 126, 483–494.
- Xu, R.H., Sampson-Barron, T.L., Gu, F., Root, S., Peck, R.M., Pan, G., Yu, J., Antosiewicz-Bourget, J., Tian, S., Stewart, R., Thomson, J.A., 2008. *NANOG* is a direct target of TGFbeta/activin-mediated SMAD signaling in human ESCs. *Cell Stem Cell* 3, 196–206.
- Yamamoto, M., Saijoh, Y., Perea-Gomez, A., Shawlot, W., Behringer, R.R., Ang, S.L., Hamada, H., Meno, C., 2004. Nodal antagonists regulate formation of the anteroposterior axis of the mouse embryo. *Nature* 428, 387–392.
- Yamamoto, M., Beppu, H., Takaoka, K., Meno, C., Li, E., Miyazono, K., Hamada, H., 2009. Antagonism between *Smad1* and *Smad2* signaling determines the site of distal visceral endoderm formation in the mouse embryo. *J. Cell Biol.* 184, 323–334.
- Yan, Y.-T., Gritsman, K., Ding, J., Burdine, R.D., Corrales, J.D., Price, S.M., Talbot, W.S., Schier, A.F., Shen, M.M., 1999. Conserved requirement for *EGF-CFC* genes in vertebrate left–right axis formation. *Genes Dev.* 13, 2527–2537.
- Yan, Y.T., Liu, J.J., Luo, Y., E.C., Haltiwanger, R.S., Abate-Shen, C., Shen, M.M., 2002. Dual roles of *Cripto* as a ligand and coreceptor in the Nodal signaling pathway. *Mol. Cell Biol.* 22, 4439–4449.
- Yeo, C., Whitman, M., 2001. Nodal signals to Smads through *Cripto*-dependent and *Cripto*-independent mechanisms. *Mol. Cell* 7, 949–957.